Cell Reports
Physical Science

CellPress
OPEN ACCESS

Perspective

Fast Charging Li-Ion Batteries for a New Era of Electric Vehicles

Matthew Li,[1] Ming Feng,[2] Dan Luo,[1] and Zhongwei Chen[1,3,*]

SUMMARY

Extreme fast charge (10 min to reach 80% state of charge) is one of the key limiting parameters preventing the widespread adoption of battery-based electric vehicles into the transportation sector. Many recent simulations and experimental-based studies have been recently published in this area with a specific focus on why extreme fast charge is challenging. These studies identified that cathode particle cracking and electrolyte transport limitation are the key barriers that have caused the well-known safety and stability problems. Interestingly, there have been very few studies that have demonstrated significant improvements toward a 10-min charge under high energy density conditions. Several strategies pertaining to electrolyte modifications (concentrated electrolyte and low viscosity additives) along with adaptive fast charging are highlighted and suggested.

INTRODUCTION

Fully battery powered electric vehicles (EVs) have become one of the most popular class of "green" vehicle.[1] Among all the factors against the widespread adoption of EVs, the relatively long charging time is arguably one of the most difficult parameters for consumers to accept and for researchers to meet. Compared to the short refueling time of internal combustion engine vehicles, the current quickest recharging time can take up to 30 min for an 80% state of charge (SOC). Achieving fast charge has been deemed as one of the most important directions for the progression of EVs in the market and, subsequently, in the field of battery science. The rate of charge of a battery is usually indicated in a unit known as C-rate. C-rate normalizes the absolute current with the capacity of the active material, resulting in a set time interval, of which the cell is expected to be a full charge or discharge. 1 C is defined as a charging time of 1 h. Previously, fast charge has been coined for charging rates of about 4 C (i.e., a theoretical 15-min charge) but less than 6 C (i.e., a theoretical 10-min charge). In practice, the complete charging protocol of EVs are never a constant current but usually switches to a constant voltage protocol nearing full charge to prevent side reactions. Therefore, a commercial EV undergoing fast charge will undergo 4 C charging up to ~80% SOC and then undergo a slower and milder constant voltage charge to reach full charge. Recent efforts to reach what is now colloquially known throughout the field as extreme fast charge (XFC) mandates a charging rate of about 6 C or greater.[2] More important and practically relevant is perhaps the obtained driving range per unit of charge time. Fast charge is up to ~320 km in 27 min (~11.85 km min^{-1} at ~135 kW) for the Tesla Supercharger station, whereas the XFC goal is a charging rate of 32 km min^{-1} at 400 kW.[3]

The ability to charge at a high current (>5 C) with thin electrodes of low energy densities is achievable, but high current charging of high energy density (thicker

[1]Department of Chemical Engineering, University of Waterloo, 200 University Ave West, Waterloo, ON N2L 3G1, Canada

[2]Key Laboratory of Functional Materials Physics and Chemistry of the Ministry of Education, Jilin Normal University, Changchun 130103, PR China

[3]Lead Contact

*Correspondence: zhwchen@uwaterloo.ca

https://doi.org/10.1016/j.xcrp.2020.100212

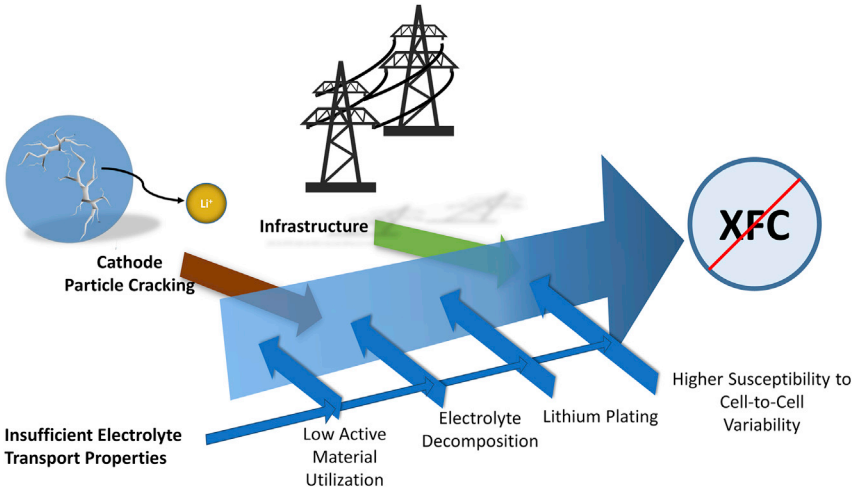

Figure 1. Problems Associated with Extreme Fast Charge
Root cause analysis of problems against extreme fast charge.

electrodes) batteries[4] and/or low temperature (<0°C)[5] is very difficult. The disadvantage of thin film battery charging is quickly realized when comparing the significantly decreased energy density (180 Wh kg^{-1} versus 220 Wh kg^{-1}) and associated cost penalty (\$196 kWh^{-1} versus \$103 kWh^{-1}) due to the increased ratio of cell deadweight material (does not contribute to charge storage) versus active material.[6] There is currently a trade-off between energy density and cost with power density. Fundamentally, all the challenges associated with XFC (at the EV level) can be succinctly reduced to a problem of mass transfer per unit area (more specifically, mass flux) or reaction kinetics.

Recent articles have focused on the status of fast charge and XFC in terms of their economics and infrastructure requirement[3,7] and battery design.[8,9] This perspective will focus on the recent analysis and the conclusion provided by leading research groups in the field. Emphasis will be placed on works that discuss key limiting phenomenon in a lithium (Li)-ion battery (LIB) during fast charge and XFC. Discussion on the Li-ion transference number will be provided along with adaptive fast charging protocols.

Key Problems Associated with XFC

Illustrating the problems associated with XFC, Figure 1 shows a root cause analysis gathered from our analysis of the literature. Overall, it appears that the insufficient electrolyte transport properties, cracking of the cathode particles, and lack of infrastructure are the key barriers against XFC. To begin, it is apparent that achieving the infrastructure required for fast charging is nontrivial. Charging rates of up to 6–9 C is taxing to the power grid. XFC or even a fast charge ports are rather rare and are currently not likely for consumers to practically find and will require significant investment from industry and government to improve. For example, in the United States, charging ports are rated as level 1, level 2, or direct current (DC) fast charging. Level 1 ports are rated for a 2- to 5-mile range per 1-h charge, level 2 stations are rated at a 10- to 20-mile range per 1 h of charge, and DC fast charging stations are rated for a 60- to 80-miles of range per 20 min of charge. As of 2019, 5% of public charging outlets are level 1, 80% are level 2, and only 15% are DC fast charging (including Tesla superchargers; CHAdeMO for Nissan, Mitsubishi, and Toyota; and combined charging system [CCS] for BMW and Chevrolet).[10] Furthermore, the current load

required from the charging facility becomes nontrivial at XFC or even at fast charge conditions and can easily disturb local power grids (voltage deviations and thermal loading)[11,12] and stress the grid[13] to the point of overloading the feeder (transmission lines from grid to charging facility).[3,7] Therefore, any breakthrough in XFC battery research much be accompanied with government support in the form of investment into enhancing the grid.

Currently, the technical problems of fast charge residing inside the battery include the following: (1) cathode particle cracking, (2) low active material utilization, (3) electrolyte-electrode side reactions, (4) Li plating at the anode. These problems are all further amplified by (5) electrode variability and are nearly all a function of insufficient mass transport properties of the cell. Below are brief descriptions of each of these problems.

Cracking of Cathode Material

Cathode materials of LIB are typically composed of agglomerated primary particles forming secondary particles. Even at relatively mild cycling currents, the secondary particles are known to crack. Specifically, intragranular cracks are formed to the nonisotropic lattice strains, as the primary particles are not arranged in any particular order in the secondary particles.[14,15] At higher Li insertion rates, the volume changes experienced by the cathode particles are further amplified, increasing heterogeneity compared to that of slower rates, and create more stress throughout the battery material.[2] This is because the Li-ion diffusion-induced stress is amplified at higher currents, such as in XFC conditions.[16,17] Surface cathode primary particles tend to have a higher SOC than the inner primary particles.[18] Cracking of the cathode material might reduce accessible Li storage sites in addition to generating more surface area for electrolyte decomposition.

Low Active Material Utilization

Fundamentally, the observed increases in cell voltages at higher charging rates is due to both thermodynamic and kinetics changes in the system. These changes stem from concentration and Li-ion transport. Due to mass transfer limitations, the concentration gradient generated in the cell at both the cathode and anode are very high. If the electrolyte Li-ion transport is the limiting step, at a higher current, the number of Li-ions generated and, as such, the Li-ion concentration at the cathode's surface will be relatively higher than the low current charging. Conversely, Li-ion concentration at the surface of the graphite will be also lower. From the mass-transfer-inclusive Butler-Volmer equation, at a given current density, the overpotential is inversely proportional to the concentration of the reduction reaction reactants. In this case, the rate of the reduction reaction of the Li-ion intercalation into the graphite anode is reduced due to the lowered Li-ion concentration, increasing the overpotential. At the same time, the different increased/decreased concentrations of Li-ion at the cathode/anode, respectively, also have a thermodynamic effect. The concentration of the Li-ion at the cathode will, on average, increase the oxidation potential required to extract Li from cathode material. At the anode's surface, the lower Li-ion concentration will push the anode down to a more reductive potential. Among other sources of overpotential (ohmic resistance, charge neutrality, etc.), the polarization experienced by both the anode and cathode increases the overall cell voltage to prematurely reach its cut-off voltage.[19] This results in the well-reported low material utilization and poor energy efficiency.

Electrolyte-Electrode Side Reaction

Under ideal conditions, the cathode and anode are passivated by cathode electrolyte interfacial (CEI) and solid electrolyte interphase (SEI), respectively, to prevent

continuous electrolyte/electrode side reactions.[20–23] However, passivation layers are imperfect and will have an area where side reactions can continue to occur. These reactions on both the cathode and anode are known to be a major battery degradation mechanism. When subjected to low currents, the side reactions are manageable due to the lower overpotentials experienced by the cathode and the anode, in addition to a likely lower operating temperature, which yields the accepted cycle life in commercial LIBs. However, at a high current density (especially under XFC conditions), the local current can be heterogeneous and might lead to significant Joule heating in the battery system due to resistance in both electron and ion flow.[24–26] The increase in temperature will increase the kinetics of side reactions (parasitic reactions) of electrolyte components with each of the electrodes.[27] At the same time, the overpotential experienced by each electrode will allow the potentials at the cathode to be more anodic and the potentials at the anode to be more cathodic, creating a larger thermodynamic driving force for these parasitic reactions. These parasitic reactions include the oxidation of electrolyte species on the cathode,[28] potential corrosion of the Al current collector,[29] and reduction of species the anode,[42] with some side reactions resulting in the generation of gaseous compounds.[27] It should be noted that there has been work that demonstrated insignificant changes to the cell temperature of a ~2-mAh cm^{-2} single-layer NMC532/graphite pouch cell charged at rates up to 9C.[2] However, this was associated with a relatively small absolute current, leading to a maximum heating rate of only 16 mW.

Li Plating

The purpose of using an N/P ratio of typically more than unity is to limit the probability of Li plating. A low N/P, that is, a high cathode-to-anode areal capacity ratio of near unity, is dangerous because it risks locally saturating the graphite anode with Li-ions and bringing the local potential past 0 versus Li^+/Li, allowing for Li plating. It should be noted that the heterogeneity in current distribution is amplified when the current is increased. At high charge rates, the overpotential experienced by the anode typically decreases the potential levels to where Li plating can occur, effectively decreasing the N/P ratio of the battery below one.[30] Li plating or the reduction of Li-ions to Li metal is particularly dangerous, as it enables the formation of Li dendrites. If the cathode and the anode were to be shorted by an internal Li dendrite, the cell is prone to undergo thermal runaway. Furthermore, the formation of metallic Li allows for the decomposition of the electrolyte. As the SEI on Li metal is unstable, the continuously formed Li (with its highly reductive nature) will constantly consume the electrolytes and generate gaseous species,[31] degrading the cycle retention of the cell if a short circuit does not occur first.

Furthermore, charging at low temperatures is well-known to cause Li plating due to the sluggish Li-ion transport in the electrolyte, leading to large overpotential at mild currents.[32] Throughout literature, this can be most effectively overcome by heating the battery from ambient to room temperature prior to any significant charging.[5] Interestingly, high temperatures were also found to facilitate Li plating, due to increases in Li-ion reduction kinetics.[33] However, this correlation between Li plating and temperature is only true if the potential experienced by the anode is low enough to thermodynamically allow for Li plating. That is, if Li plating were to occur, a high operating temperature will likely speed up the rate of dendrite growth.

High Susceptibility to Cell-to-Cell Variability

Overarching these problems is the amplification effect of any variability in the cell's physical characteristics.[16] Any spatial heterogeneity in the electrode could serve as a point of higher or lower current (depending on its local pressure), which could

amplify the effective local current beyond even the highly demanding XFC conditions. Furthermore, heterogeneity in the form of binder/carbon black and active material aggregates has been suggested to have a significant impact under XFC conditions. Aggregates tends to have more active material per volume but also lower mass transfer rates, leading to a preferential lithiation/delithiation from a low to high degree of aggregation.[34] Together, they will increase damage to the cell through either a decreased cycle life or complete cell failure. Therefore, the manufacturing of XFC cells will demand an even higher design to prevent any slight variability in the cells. It should be noted that so-called secondary pore networks that are designed to provide more efficient Li-ion transport highways could have in-plane columns of electrodes that could potentially and mistakenly serve as a point of higher contact pressure and, as such, an undesirable higher local current.

Strategies and Problems with Strategies

Numerous strategies have been investigated to alleviate the limitation of fast charge and XFC. They include heat management,[5,35–39] electrode architecture design,[40,41] material design,[42–44] electrolyte formulation,[45–47] and charging protocol.[48–50] In general, all of these techniques attempt to relieve the following mass transfer limitations of LIBs: (1) to achieve high current and (2) to maintain cell reversibility over prolonged cycling. Heat management revolves around the concept of heating the cell to ensure higher Li-ion conductivity, while ensuring the cell does not overheat by cooling. This technique yielded dramatic improvement in charging under cold ambient conditions. However, cycle life at elevated temperatures will inevitably lead to higher side reaction between the electrode and electrolyte. Electrode architecture design entails the reduction in the tortuosity of the cell. This includes using spherical particles,[24] larger particles, electrode pore templating, and even diffusion channel milling with a laser. Electrolyte formulations have focused on achieving higher transport properties in both ionic conductivity and Li-ion transference number by decreasing the mobility of the anion.[45,46,51] Finally, charging protocol is a technique that is probably the least invasive and provides enormous options toward XFC.[52] Table 1 provides a brief overview of some of the highest performances from each of the strategies, along with some comment on their disadvantages and future outlooks.

The possible problems of fast charge of XFC are easily listed and conceptually simple, reducing to ultimately a problem of mass transfer and reaction kinetics to certain parts of the cell. However, like any rate-dependent process, the key rate-determining step is the most impactful to the overall cell overpotential. Although many of the aforementioned mitigation strategies have looked into enhancing different parts of the cells (all with interesting improvements in rate performance), only recently have researchers begun to identify the components of total cell overpotential that are likely mostly responsible for the observed poor performance metrics.[30] A collaborative and rather comprehensive work by National Renewable Energy Laboratories (NREL), Argonne National Laboratories (ANL), and Idaho National Laboratories (INL) has identified that Li-ion transport in the electrolyte is the key culprit against XFC.[4,6] Experimental results revealed that XFC even up to 9 C did not sacrifice much energy density or promote Li plating for thin film electrodes in a pouch cell. These cells were designed to be ~1.5 mAh cm^{-2}, with a thickness of 42 μm, porosity of 33%, and total areal of 14.1 cm^2 for the cathode, and ~2 mAh cm^{-2}, with a thickness of 47 μm, porosity of 37%, and areal of 14.9 cm^2 for the anode (N/P = 1.13). At 8 C, the low loading cells were able to reach almost 70% SOC (Figure 2A). This suggests that the material itself is not that poorly suited for lithiation up to 9 C. In contrast, higher areal loading cells of about 2.5 mAh cm^{-2} for cathode and 3 mAh cm^{-2} for anode achieved less than 20% SOC at 8 C (Figure 2B). This was well

Table 1. Overview of Strategies for Fast Charge

Areal active/ capacity loading	Capacity versus C-rate	Testing conditions	Method	Disadvantage	Outlook	Reference
Cathode: 1.5 mAh cm^{-2}	Single-layer pouch full cell:	Anode: 47-μm thick (37% porosity), 14.9 cm^{-2} graphite	Baseline (i.e., no particular modification)	Low energy density and high cost	Limited application	6
Anode: 2 mAh cm^{-2}	1 C: 19 mAh	Cathode: 42-μm thick (33% porosity), 14.1 cm^{-2}				
	6 C: 13.5 mAh	NMC532				
	8 C:~12.9 mAh	N/P = 1.13				
		Electrolyte:GEN 2				
		Temperature:30°C				
Cathode: 2.5 mAh cm^{-2}	Single-layer pouch full cell:	Anode: 70-μm thick (35% porosity) graphite				
Anode: 3 mAh cm^{-2}	1 C:32 mAh	Cathode:71-μm thick (35% porosity)				
	6 C:12.32 mAh	NMC532				
	8 C:5.76 mAh	N/P = 1.07				
		Electrolyte:GEN 2				
		Temperature:30°C				
2.35 mAh cm^{-2}	Single-layer pouch full cell: CC to 4.2 V then CV at 4.2 until the theoretical charge time dictated by C-rate	Anode: 8 mg cm^{-2} (30% porosity) graphite	Substituting $LiPF_6$ with LiFSI with higher Li-ion transference number	Higher cost	Require synthesis of cheaper Li salt with high Li transference number	46
	$LiPF_6$:	Cathode: 14.1 mg cm^{-2} (30% porosity)				
	1 C: 170.8 mAh g^{-1}	NMC811				
	5 C: 135.4 mAh g^{-1}	N/P = 1.106				
	LiFSI:	Electrolyte: 1.5 $LiPF_6$ or LiFSI in 30:70 weight ratio EC:EMC.				
	1 C: 173.8 mAh g^{-1}	Temperature: 30°C				
	5 C: 153.2 mAh g^{-1}					
5 mg cm^{-1} (~1.86 mAh cm^{-2})	Coin half cell:	Working electrode: 200 μm (for 9.1 mg cm^{-1}) Graphite	Magnetic alignment of graphite	Rate performance not significantly enhanced	Performance benefit appears to be not significant when considering the amount of change to the manufacturing process that is required	81
	0.1 C:372 mAh g^{-1}	Li metal reference electrode	Pore structure optimization			
	1 C:160 mAh g^{-1}	Electrolyte: 1M $LiPF_6$ 1:1 weight, EC: DMC				
9.1 mg cm^{-2} (3.6 mAh cm^{-2})	1 C:83 mAh g^{-1}	Temperature: 25°C				
2.5 mAh cm^{-2}	Coin 0.1 C: 2.5 mAh cm^{-2}	Anode: 64-μm thick (35% porosity), graphite	Laser milling	Likely very expensive to scale up	Performance benefit appears to be not significant when considering the amount of change to the manufacturing process that is required	82
	1 C: ~2.35mAh cm^{-2}	Cathode: 64-μm thick (35% porosity), NMC111				
	3 C: ~1.75 mAh cm^{-2}	N/p = 1.2				

(*Continued on next page*)

Table 1. *Continued*

Areal active/ capacity loading	Capacity versus C-rate	Testing conditions	Method	Disadvantage	Outlook	Reference
	5 C: 1 mAh cm^{-2}	Electrolyte: 1M $LiPF_6$ +2% VC 3:7: weight ratio EC:EMC				
		Temperature = 20°C				
2.5 mAh cm^{-2}	All constant current at 6 C then CV, with a total time of 10 min:	Anode: 70-μm thick (35% porosity) graphite	Temperature elevation	Will likely expedite electrolyte degradation	Will likely require an electrolyte with higher resistance to oxidation and reduction at elevated temperatures	6
	30°C:36%(CC)+43%(CV) = 79%SOC	Cathode: 71-μm thick (35% porosity)				
	40°C:38%(CC)+43%(CV) = 81%SOC	NMC532				
	50°C:52%(CC)+35%(CV) = 87%SOC	N/P = 1.07				
		Electrolyte: GEN 2				
		Temperature: varies				
6 mg cm^{-2} (~1,100 mAh g^{-1} @ 0.2 C)	2 C = ~4 mAh cm^{-2}	Anode versus lithium metal half cell	Graphene particles	Scalability of graphene-based particles might be low	Scalability is usually overlooked in exotic material design and must be considered carefully in future studies, but performance appears promising	24
	5 C = ~3.25 mAh cm^{-2}	Mesoporous graphene particles				
	10 C = ~2.85 mAh cm^{-2}	Electrolyte: 4M lithium bis(fluorosulfonyl) imide in 1,2-dimethoxyethane				
N/A	4.4 C→5.6 C→5.2 C→4.252 C	Anode: 40 μm, graphite	Machine learning-optimized charging protocol	Only a mitigation and optimization strategy and does not introduce any distinct change to the system	If coupled correctly with more input based on operando characterization techniques, this could be more impactful	74
	1 C = 1.1 A	Cathode: 80 μm $LiFePO_4$				
		A123 APR18650M1A cells rated for 1.1 Ah and 3.3 V				

reproduced by their mathematical model, which considered the lithiation state of nickel-manganese-cobalt (NMC) and graphite particles and the tortuosity of the cell. The simulated Li-ion concentration in the electrolyte was shown to increase as one move from the anode to the cathode for low loading (Figure 2C) and high loading cells (Figure 2D), which is reasonable, as the Li-ion comes from the cathode. This variation in concentration was found to be exaggerated at higher currents for both higher and lower loading cells. Specifically, the Li-ion concentration decreases to near zero at the current collector of the anode, whereas the Li-ion increases to over 3 M near the current collector of the cathode. It is worth noting that 2.5 mAh cm^{-2} is still well below the standard for what is considered high energy density cells (4–5 mAh cm^{-2}). Furthermore, the SOC of the cathode and anode under thin (Figure 2E) and thick film (Figure 2F) conditions revealed a lack of lithiation (graphite)/delithiation (NMC) as one move from the electrode portion closest to the separator toward their respective current collectors during fast charge. This has been also corroborated by operando X-ray diffraction studies with in-plane spatial resolution where lithiation states at the end of charge were well below ~40% for graphite near the current collector.[53] Taken together, this evidence suggests that the drastic

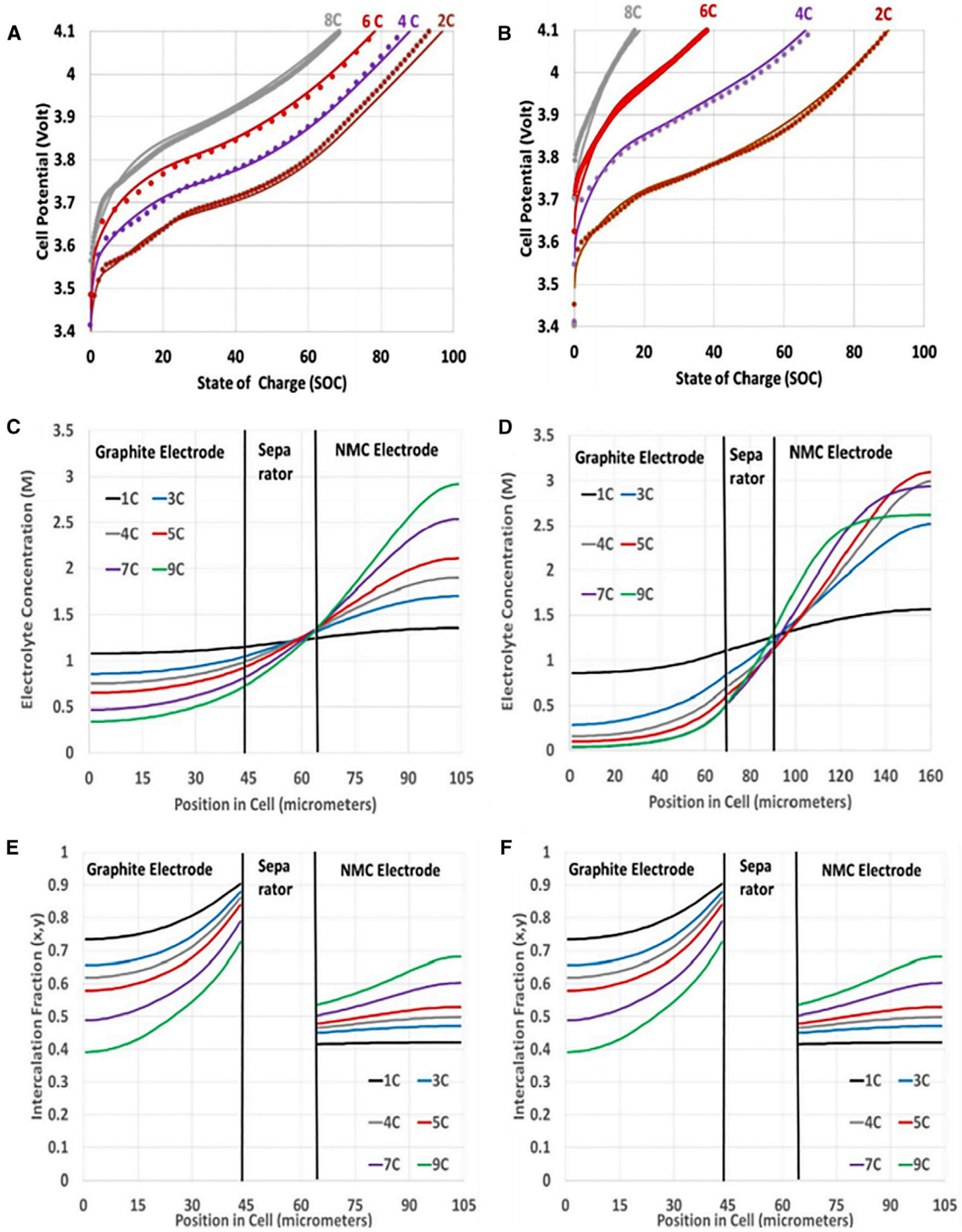

Figure 2. Simulated Cells under Extreme Fast Charge Conditions

Experimental and simulated voltage profile at various C-rates of thin (A) and thick (B) loading cells. Simulated concentration profiles as a function of cell length at various C-rates of thin (C) and thick (D) loading cells. Simulated lithiation state as a function of cell length at various C-rates of thin (E) and thick (F) loading cells. Reproduced with permission.[6] Copyright Elsevier 2020.

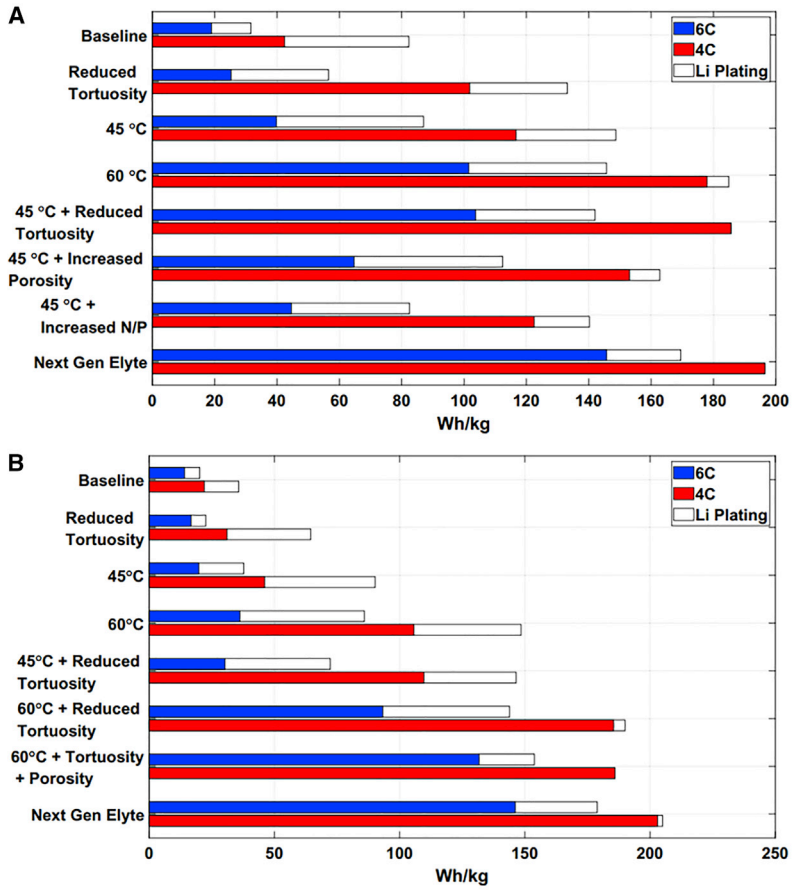

Figure 3. Projected Energy Density from NREL/ANL/INL Model under Various Hypothetical Cell Conditions

Simulated at 3 (A) and 4 (B) mAh cm^{-2}. Colored portions of the bars represent safe achievable energy density by a constant current protocol, and the white bars represent remaining achievable energy density but with a high likelihood of Li plating. Reproduced with permission.[6] Copyright Elsevier 2020.

difference in performance was concluded to be mostly associated with a lack of Li-ion transport in the electrolyte.

Perhaps the more interesting research was the hypothetical scenarios of enhanced performance conditions studied by this work. By modeling the cells at various tortuosity, cell porosity, temperature, electrolyte transference number, and N/P ratio and a combinations of these parameters, the authors were able to forecast the expected point of SOC that will drop the potential at any spatial point in the electrode to allow for Li plating, as shown in Figures 3A and 3B (at 3 and 4 mAh cm^{-2}, respectively). According to their simulation, for the 3-mAh cm^{-2} cell, the decrease of cell tortuosity at 45°C has a large impact on delaying the Li plating SOC and matches the effect of charging at 60°C. Increasing temperature appears to be a promising avenue for XFC, but its effect on cycle stability is likely negative. Changes to the N/P ratio was found to not have much of an effect on the performance. Cells simulated at 45°C did not have significant improvement in Li plating SOC when the N/P ratio was increased. This is likely because Li plating is very much a localized mass transport phenomenon at high currents and not necessarily related to the overall average SOC of the cell. N/P ratios only serve to ensure that the average equilibrium potential of

the anode stays above Li plating, such that overpotentials at low current do not drop the potential below 0 versus Li^+/Li. The results presented here indicate that the overpotential experienced by the anode at 4–6 C is probably much larger than the average thermodynamic "buffer room" offered by the increasing N/P ratio. Interestingly, when the simulated loading was increased to 4 mAh cm^{-2} (typical level for high energy density cells), many of the benefits of increasing tortuosity and temperature were decreased, especially at 6 C. Specifically, the Li-metal-free plating at 6 C at 45°C was only slightly improved compared to the baseline. This is critical, as it indicates that most of the possible techniques (which also come at the cost of different performance metrics, i.e., stability) might taper off at high energy density loadings.

In contrast, there appears to be an enormous benefit of increasing the Li-ion transference number (t^+_{Li}) and diffusivity in the electrolyte. Shown in Figures 3A and 3B the "Next Gen Electrolyte" represents a situation in which a hypothetical electrolyte has increased transport properties (1.8 times the normal ionic conductivity = 18 mS cm^{-1}, 3 times the normal diffusivity = 5 × 10^{-6} cm^2 s^{-1}, and 0.05 improvement in t^+_{Li} to 0.51 at 3 mAh cm^{-2}). Even higher transport properties were used for the hypothetical electrolyte in the simulation at 4 mAh cm^{-2} (2.3 times the ionic conductivity = 23 mS cm^{-1}, 4 times the diffusivity = 6.67 × 10^{-6} cm^2 s^{-1}, and 0.15 increase in t^+_{Li} to 0.65). This indicates that the discovery of a cost-effective electrolyte with a high Li-ion transference number might outperform all of and combinations of the other investigated parameters. The t^+_{Li} describes the portion that are carried by Li-ions and allows for one to quantify the effective conductivity that is actually useful for a LIB (Li-ion transport). During charge (an imposed electric field), Li-ions are transported from the cathode to the anode, while anions are transported toward the cathode. Transference numbers far below unity indicate that a significant portion of charge transport is carried by the anion, which does not react appreciably (in comparison to Li-ions) with the electrodes. In fact, the movement of anions leads to anion concentration build up at the cathode and would cause Li-ions to be attracted backward (due to charge neutrality) toward the cathode, leading to the generation of unfavorable and significant concentration gradients. Ultimately, this significantly deteriorates/lags Li-ion transport and has been identified to expedite Li dendrite formation in Li metal batteries.[54] The impact of t^+_{Li} can be easily seen in Figure 4A, where a t^+_{Li} of 0.8 was simulated (based on the Newman model with a porous $LiCoO_2$ cathode and porous graphite anode) to be able to reach a SOC of ~50% at 4 C. In contrast, a t^+_{Li} of 0.4 was projected to only reach <30%. The difference is more apparent when moving up to a t^+_{Li} of 1 and charging rate of 6 C (XFC). It is important to note that conductivity must be maintained to be reasonably high to observe the benefit of a high t^+_{Li}. The relationship between t^+_{Li}, diffusivity (proportional to viscosity of electrolyte), and ionic conductivity have been practically very close. Increasing one usually sacrifices another, and their relationships are not always clear experimentally due to difficulty in measurement of their values. Perhaps more important instead is their actual impact on the performance in reaching an appreciable SOC. Specifically, the trade-offs and impact on the overall performance in terms of the achievability of a 75% SOC at 2 C can be found in Figure 4B. At low t^+_{Li}, the diffusion coefficient (D_{o+}) has a large influence on the required overall conductivity to achieve 75% SOC. By decreasing D_{o+} from 2.5 × 10^{-6} to just 2.0 × 10^{-6} cm^2 s^{-1} (20% decrease) at a t^+_{Li} of 0.6, the required conductivity increase to compensate is from ~6.8 to ~9.2 mS cm^{-1}. At a high t^+_{Li} (0.9), the compensation in ionic conductivity is significantly reduced with only a requirement of an increase from ~4.4 to 4.6 mS cm^{-1}.

Research efforts has been currently funneled toward ways to limit the mobility of anions. Currently, the popular methods include chemically tethering anions in polyelectrolyte/ionomers[55] and onto nanoparticles[56] and the synthesis of large anions

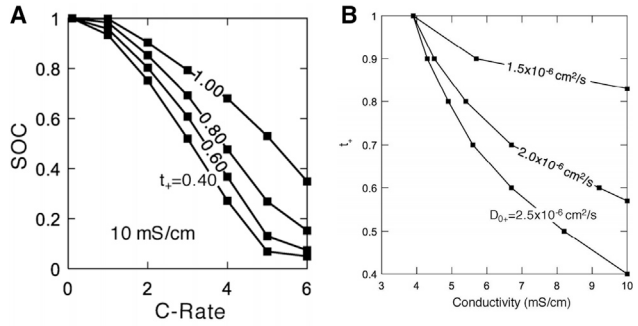

Figure 4. Effect of Electrolyte Properties on Performance

State of charge (SOC) achievable as a function of C-rate and Li-ion transference number with an electrolyte overall conductivity of 10 mS cm^{-1} (A), and contour plots of simulated cells reaching a 2 C charge rate reaching an overall 75% SOC as a function of Li-ion diffusivity D_{0+}, overall conductivity, and Li-ion transference number (B). Both studies were simulated using a 91.8-μm-thick graphite anode and 100-μm-thick $LiCoO_2$ cathode. Reproduced with permission.[60] Copyright American Chemical Society 2017.

that have very poor mobility[57] and concentrated electrolytes.[58] However, the significant impact of the t^+_{Li} on high power and energy density batteries has been known for decades.[59] A literature survey by McCloskey et al.[60] indicated that many of the published single-ion conductor systems (near unity t^+_{Li}) usually suffer from very poor overall conductivity (<0.03 mS cm^{-1} at 30°C). Currently, it appears that one of the most promising directions for high t^+_{Li} is concentrated electrolytes with a high t^+_{Li} of 0.73 and overall conductivity of ~3.2 mS cm^{-1}.[58] Even with their commonly significantly higher viscosities, currents of up to 10 mA cm^{-2} have been demonstrated for these types of electrolyte systems, albeit for an Li metal anode with unclear SOC.[61] In addition to the significantly increased mass density of the electrolyte, one of the key problems is the high cost penalty of using a concentrated electrolyte with expensive salts, such as the popular LiTFSI.[24,62,63] Of all the cell components, the cost of the electrolyte amounts to about 6%–9.9% (~35 USD kWh^{-1} at 22 USD L^{-1} with 1.6 $L_{elecrolyte}$ kWh^{-1} in 2015) of the total cost (~580 USD kWh^{-1} in 2015),[64–66] which assumes a price of about ~85 USD kg^{-1} (15.6 USD $L^{-1}_{electrolyte}$) for $LiPF_6$ if the other components (6.4 USD $L^{-1}_{electrolyte}$ for combined EC and DEC) were assumed to be at ~1.3 and 2.1 USD kg^{-1}, respectively.[67] A recent study performed at ANL indicated that the cost of $LiPF_6$ produced at a plant of 10 kt $year^{-1}$ capacity could be as low as 20 USD kg^{-1} (in 2019) if the chemical process was optimized.[67] This would yield a total $LiPF_6$ cost of ~3.7 USD $L^{-1}_{electrolyte}$, which would decrease the overall cost of electrolyte to be ~10 USD $L^{-1}_{electrolyte}$, including all components. The cost of LiTFSI or LiFSI (commonly used in concentrated systems[23]) are about 100 USD kg^{-1},[68] forecasting a cost of 28.71 and 18.7 × molarity of salt USD $L^{-1}_{electrolyte}$, respectively. If the concentrations were to even venture conservatively into the "concentrated-electrolyte" regime (4.5 M), the cost would be ~129 (LiTFSI) and ~84 (LiFSI) USD $L^{-1}_{electrolyte}$, respectively, just for the salt. Assuming the required electrolyte proportions (~1.6 $L_{electrolyte}$ kWh^{-1}) in prospective fast charge LIBs were not increased, the total cost can be estimated to be 206 and 135 USD kWh^{-1}, respectively (without solvent).

Putting our brief analysis into perspective, when compared to the conservative (dated) cost of GEN 2, $LiPF_6$, and solvent-included electrolyte at 35 USD kWh^{-1} (2015), the cost increase is quite substantial and will probably at least double any 2020 estimates of total battery cost. Even in 2018, the cost of LIB for EVs have been already drastically reduced from ~580 USD kWh in 2015 to well below

280 USD kWh^{-1} (2018).[22] This suggests that if a 4.5 M LiTFSI solution was to be used in substitution of typical GEN 2 (at most 35 USD kWh^{-1}), it would already increase the cost of LIBs by nearly two-thirds (from <280 to ~451 USD kWh^{-1}). With economies of scale and optimization, the cost of these electrolyte salts will without a doubt decrease, but it is unclear to what level, as the cost of the high concentration of salt entails a substitution for solvent. Enhancing the transport properties of the electrolyte with both a higher ionic conductivity and near unity Li-ion transference number is difficult. Finding or synthesizing such a salt while achieving a similar or reduced price compared to $LiPF_6$ and, more importantly, the solvents (at higher concentrations) will be an even more challenging task.

Tuning the viscosity of the electrolyte as a means of increasing the diffusivity of Li-ions and, as such, the ionic conductivity appears to be more appealing.[51,63] Logan et al.[69] indicated that a significant enhancement in conductivity can be achieved if methyl acetate (low viscosity liquid ~0.38 cP at 20°C) was mixed into the electrolyte (viscosity of about 3.5 cP at 20°C). At 30% weight % in the solvent (30% EC, 40% DMC), the conductivity increased from 11 mS cm^{-1} (3.5 cP) to ~15.3 mS cm^{-1} (2.4 cP) at 20°C, which is nearing the Next Gen Electrolyte levels. In fact, the ionic conductivity can be mostly estimated from the viscosity by the Walden rule in which viscosity is inversely proportional to conductivity. However, the cycle stability of methyl acetate and other low-viscosity lighter molecular weight solvents tend to be poor, as they were often found to not form stable SEI layers.[70]

Looking beyond battery design, adaptive fast charging protocols in which currents are precisely controlled as a function of measured cell characteristics can be a very attractive methodology for achieving fast charge. Localized sensor design can be used to accurately measure local electrode temperatures[71] and SOC[72] to enable a more accurate and appropriate control of current. One of the most illustrative plots of the different components of overpotential imparted onto the cell by inefficiencies is the Nyquist and Bode plots obtained from electrochemical impedance spectroscopy (EIS).The different timescales of various mass and charge transport phenomenon can be deconvoluted to a very high degree by using EIS. Potentiostatic EIS that is an AC oscillation about a null current used to investigate permanent changes to the impedance is crucial to understand aging mechanism of XFCs. The main downside of this technique is the fact that there is no net current through the cell and the test is required to be performed at near-equilibrium conditions that is usually achieved by resting the cells before taking the EIS spectrum. These two requirements coupled together could allow the cell to relax the conditions that caused the large overpotential during XFC. In contrast, dynamic EIS that is an alternating current (AC) oscillation superimposed over a constant current can be used to investigate online impedance sources that might be useful to isolate mass transfer limitations.[73] Together, both of these techniques can be very useful as input data into a learning model.

Currently, the use of a data-driven approach to optimize the battery charging protocol for reaching a total charge time that is considered XFC will likely begin to play an enormous role in the field. One can imagine that a charging protocol with input parameters of voltage or current can be finely tuned based on the characteristic (temperature, voltage, and SOC) readings to build a battery management system that can efficiently maximize the achievable SOC (without damage to the cell) within a set amount of time. Machine learning (ML)-based techniques have already shown the battery community some surprising results in the charging protocols explored by researchers.[74] Many groups have demonstrated that decreasing the current

with increasing SOC is an effective method toward limiting Li plating.[75,76] However, ML has demonstrated that the top three (ranked based on cycle stability) charging protocols do not always follow this rule, with one particular protocol entailing a current charging pattern of 4.4 C→5.6 C→5.2 C→4.252 C, yielding a very high cycle life performance. Based on this information, the authors speculated that the parasitic reactions caused by heat generation might be more important for enhancing cycle life rather than Li plating. If more accurate and detailed onboard sensors could be inserted into the cell, more localized parameters can be measured and their respective correlations with performance could be very impactful for designing a charge protocol. Simultaneous variations in the charge protocol while also changing, for example, tortuosity and porosity of the cells have not, to the best of our knowledge, been explored and could lead to significant compounded performance enhancements.

Conclusions and Perspectives

This perspective has briefly summarized some of the key problems and strategies for fast charging LIBs. Furthermore, we have presented in more detail the limitations and pitfalls of some of these proposed strategies. From recent works, it appears that (besides the problem of cathode cracking) the key limiting factor associated with XFC can be succinctly reduced to a problem of transporting Li-ion efficiently through the electrolyte. Addressing this problem could mitigate/reduce many of the subsequently associated problems (low material utilization, Li-plating, electrolyte/electrode side reactions, and higher susceptibility to inhomogeneous electrode). Highly concentrated electrolytes could indeed increase the Li-ion transference number but would come at the cost of viscosity, an increase in electrolyte mass density, and an increase in cost. Conversely, the use of lighter and less viscous electrolyte solvents might be able to increase the transport properties of the electrolyte, but they usually result in poor cycle stability. Furthermore, the cracking of the cathode has been established as a key problem in achieving XFC with high cycle life. Surprisingly, although there have been a few works[18,23,24] that discuss the failure mode of cathode particles, the amount of papers associated with achieving XFC (reducing radial SOC gradients) for cathode particles has been low.

Among all the discussed techniques, it is relatively simple to sacrifice energy density for power. A thinner electrode will naturally fair better under XFC conditions than a thick electrode. Practically, this idea has been somewhat dismissed due to the increased cost and reduced energy density associated with more deadweight material in the battery pack. However, there has been recent commercial interest by Tesla to switch to Li-iron-phosphate-based cathodes in some markets.[77] In fact, if Li-iron phosphate cathodes (safer and cheaper) are considered, the restrictions for space optimization in regard to safety, cost, and range could potentially be relaxed and the subsequent more compact battery packing system designs could be used to compensate for thinner electrodes.

Finally, the goal of fast charge is fundamentally limited, in many aspects, by the transport properties of the electrolyte, which are extremely challenging to enhance and will require a significant breakthrough in electrolyte design and synthesis. This is further complicated by the strict cost requirement of any newly synthesized electrolyte chemicals. Conversely, two main methods of achieving XFC are particularly intriguing. First, the adaptive fast charging techniques, which consist of a feedback loop of various onboard characterizations (e.g., temperature and SOC) coupled with a variable current protocol, appear to be very interesting. This technique is still, nevertheless, an optimization of the LIB system, and it is unclear if it can ever be

significantly enhanced to XFC levels. The standardization of battery packs among different manufacturers of EVs will significantly alter the possibly of a battery swapping station. The logistics of the standardization might already be heavily considered by EV companies and government from both an environmental perspective (especially with pushes toward increased volume of LIB recycling) and faster refuel times by battery swapping stations. Battery swapping stations have been already tested in Taiwan (albeit for electric scooters for which the size of the battery is much smaller).[78,79] These stations entail the standardization of battery packs along with a stock of readily charged batteries available to consumers who drive up to the station and swap out their battery pack.[80]

ACKNOWLEDGMENTS

The authors would like to acknowledge support from the Natural Sciences and Engineering Research Council of Canada (NSERC) of Canada, Waterloo Institute for Nanotechnology, University of Waterloo, and the University of Waterloo.

AUTHOR CONTRIBUTIONS

All authors contributed to the writing and content of this work.

DECLARATION OF INTERESTS

The authors declare no conflict of interest.

REFERENCES

1. Duan, J., Tang, X., Dai, H., Yang, Y., Wu, W., Wei, X., and Huang, Y. (2020). Building Safe Lithium-Ion Batteries for Electric Vehicles: A Review. Electrochemical Energy Reviews *3*, 1–42.

2. Tanim, T.R., Dufek, E.J., Evans, M., Dickerson, C., Jansen, A.N., Polzin, B.J., Dunlop, A.R., Trask, S.E., Jackman, R., Bloom, I., et al. (2019). Extreme Fast Charge Challenges for Lithium-Ion Battery: Variability and Positive Electrode Issues. J. Electrochem. Soc. *166*, A1926–A1938.

3. Burnham, A., Dufek, E.J., Stephens, T., Francfort, J., Michelbacher, C., Carlson, R.B., Zhang, J., Vijayagopal, R., Dias, F., Mohanpurkar, M., et al. (2017). Enabling fast charging—Infrastructure and economic considerations. J. Power Sources *367*, 237–249.

4. Colclasure, A.M., Dunlop, A.R., Trask, S.E., Polzin, B.J., Jansen, A.N., and Smith, K. (2019). Requirements for Enabling Extreme Fast Charging of High Energy Density Li-Ion Cells while Avoiding Lithium Plating. J. Electrochem. Soc. *166*, A1412–A1424.

5. Yang, X.G., Zhang, G., Ge, S., and Wang, C.Y. (2018). Fast charging of lithium-ion batteries at all temperatures. Proc. Natl. Acad. Sci. USA *115*, 7266–7271.

6. Colclasure, A.M., Tanim, T.R., Jansen, A.N., Trask, S.E., Dunlop, A.R., Polzin, B.J., Bloom, I., Robertson, D., Flores, L., Evans, M., et al. (2020). Electrode scale and electrolyte transport effects on extreme fast charging of lithium-ion cells. Electrochim. Acta *337*, 135854.

7. Srdic, S., and Lukic, S. (2019). Toward Extreme Fast Charging: Challenges and Opportunities in Directly Connecting to Medium-Voltage Line. IEEE Electrification Mag. *7*, 22–31.

8. Liu, Y., Zhu, Y., and Cui, Y. (2019). Challenges and opportunities towards fast-charging battery materials. Nat. Energy *4*, 540–550.

9. Zhu, G.-L., Zhao, C.-Z., Huang, J.-Q., He, C., Zhang, J., Chen, S., Xu, L., Yuan, H., and Zhang, Q. (2019). Fast Charging Lithium Batteries: Recent Progress and Future Prospects. Small *15*, e1805389.

10. Developing Infrastructure to Charge Plug-In Electric Vehicles https://afdc.energy.gov/fuels/electricity_infrastructure.html.

11. Sehar, F., Pipattanasomporn, M., and Rahman, S. (2017). Demand management to mitigate impacts of plug-in electric vehicle fast charge in buildings with renewables. Energy *120*, 642–651.

12. Yong, J.Y., Ramachandaramurthy, V.K., Tan, K.M., and Mithulananthan, N. (2015). A review on the state-of-the-art technologies of electric vehicle, its impacts and prospects. Renew. Sustain. Energy Rev. *49*, 365–385.

13. Dharmakeerthi, C.H., Mithulananthan, N., and Saha, T.K. (2014). Impact of electric vehicle fast charging on power system voltage stability. Int. J. Elec. Power *57*, 241–249.

14. Liu, H., Wolf, M., Karki, K., Yu, Y.-S., Stach, E.A., Cabana, J., Chapman, K.W., and Chupas, P.J. (2017). Intergranular Cracking as a Major Cause of Long-Term Capacity Fading of Layered Cathodes. Nano Lett. *17*, 3452–3457.

15. Deng, S., Li, X., Ren, Z., Li, W., Luo, J., Liang, J., Liang, J., Banis, M.N., Li, M., Zhao, Y., et al. (2020). Dual-functional interfaces for highly stable Ni-rich layered cathodes in sulfide all-solid-state batteries. Energy Storage Mater. *27*, 117–123.

16. Lim, C., Yan, B., Yin, L., and Zhu, L. (2012). Simulation of diffusion-induced stress using reconstructed electrodes particle structures generated by micro/nano-CT. Electrochim. Acta *75*, 279–287.

17. Xia, S., Mu, L., Xu, Z., Wang, J., Wei, C., Liu, L., Pianetta, P., Zhao, K., Yu, X., Lin, F., and Liu, Y. (2018). Chemomechanical interplay of layered cathode materials undergoing fast charging in lithium batteries. Nano Energy *53*, 753–762.

18. Liu, T., Du, Z., Wu, X., Rahman, M.M., Nordlund, D., Zhao, K., Schulz, M.D., Lin, F., Wood, D.L., and Belharouak, I. (2020). Bulk and Surface Structural Changes in High Nickel Cathodes Subjected to Fast Charging Conditions (ChemComm).

19. Richardson, G.W., Foster, J.M., Ranom, R., Please, C.P., and Ramos, A.M. (2020). Charge transport modelling of Lithium ion batteries. arXiv, 00806, arXiv.

20. Wang, Z., Lee, J.Z., Xin, H.L., Han, L., Grillon, N., Guy-Bouyssou, D., Bouyssou, E., Proust, M., and Meng, Y.S. (2016). Effects of cathode electrolyte interfacial (CEI) layer on long term cycling of all-solid-state thin-film batteries. J. Power Sources *324*, 342–348.

21. An, S.J., Li, J., Daniel, C., Mohanty, D., Nagpure, S., and Wood, D.L. (2016). The state of understanding of the lithium-ion-battery graphite solid electrolyte interphase (SEI) and its relationship to formation cycling. Carbon *105*, 52–76.

22. Li, M., Lu, J., Chen, Z., and Amine, K. (2018). 30 Years of Lithium-Ion Batteries. Adv. Mater. *2018*, e1800561.

23. Li, M., Wang, C., Chen, Z., Xu, K., and Lu, J. (2020). New Concepts in Electrolytes. Chem. Rev. *120*, 6783–6819.

24. Mo, R., Li, F., Tan, X., Xu, P., Tao, R., Shen, G., Lu, X., Liu, F., Shen, L., Xu, B., et al. (2019). High-quality mesoporous graphene particles as high-energy and fast-charging anodes for lithium-ion batteries. Nat. Commun. *10*, 1474.

25. Kang, T., Park, S., Lee, P.-Y., Cho, I.-H., Yoo, K., and Kim, J. (2020). Thermal Analysis of a Parallel-Configured Battery Pack (1S18P) Using 21700 Cells for a Battery-Powered Train. Electronics (Basel) *9*, 447.

26. Koo, B., Yi, J., Lee, D., Shin, C.B., and Park, S. (2018). Modeling the Effect of Fast Charge Scenario on the Cycle Life of a Lithium-Ion Battery. J. Electrochem. Soc. *165*, A3674–A3683.

27. Chang, W., Bommier, C., Fair, T., Yeung, J., Patil, S., and Steingart, D. (2020). Understanding Adverse Effects of Temperature Shifts on Li-Ion Batteries: An Operando Acoustic Study. J. Electrochem. Soc. *167*, 090503.

28. Zeng, X., Xu, G.-L., Li, Y., Luo, X., Maglia, F., Bauer, C., Lux, S.F., Paschos, O., Kim, S.-J., Lamp, P., et al. (2016). Kinetic Study of Parasitic Reactions in Lithium-Ion Batteries: A Case Study on $LiNi_{(0.6)}Mn_{(0.2)}Co_{(0.2)}O_2$. ACS Appl. Mater. Interfaces *8*, 3446–3451.

29. Li, X., Deng, S., Banis, M.N., Doyle-Davis, K., Zhang, D., Zhang, T., Yang, J., Divigalpitiya, R., Brandys, F., Li, R., and Sun, X. (2019). Suppressing Corrosion of Aluminum Foils via Highly Conductive Graphene-like Carbon Coating in High-Performance Lithium-Based Batteries. ACS Appl. Mater. Interfaces *11*, 32826–32832.

30. Mao, C., Ruther, R.E., Li, J., Du, Z., and Belharouak, I. (2018). Identifying the limiting electrode in lithium ion batteries for extreme fast charging. Electrochem. Commun. *97*, 37–41.

31. Liu, Q.Q., Xiong, D.J., Petibon, R., Du, C.Y., and Dahn, J.R. (2016). Gas Evolution during Unwanted Lithium Plating in Li-Ion Cells with EC-Based or EC-Free Electrolytes. J. Electrochem. Soc. *163*, A3010–A3015.

32. Campbell, I.D., Marzook, M., Marinescu, M., and Offer, G.J. (2019). How Observable Is Lithium Plating? Differential Voltage Analysis to Identify and Quantify Lithium Plating Following Fast Charging of Cold Lithium-Ion Batteries. J. Electrochem. Soc. *166*, A725–A739.

33. Zhu, Y., Xie, J., Pei, A., Liu, B., Wu, Y., Lin, D., Li, J., Wang, H., Chen, H., Xu, J., et al. (2019). Fast lithium growth and short circuit induced by localized-temperature hotspots in lithium batteries. Nat. Commun. *10*, 2067.

34. Mistry, A., Smith, K., and Mukherjee, P.P. (2020). Stochasticity at Scales Leads to Lithium Intercalation Cascade. ACS Appl. Mater. Interfaces *12*, 16359–16366.

35. Ye, Y., Shi, Y., Saw, L.H., and Tay, A.A.O. (2016). Performance assessment and optimization of a heat pipe thermal management system for fast charging lithium ion battery packs. Int. J. Heat Mass Transf. *92*, 893–903.

36. Prada, E., Di Domenico, D., Creff, Y., Bernard, J., Sauvant-Moynot, V., and Huet, F. (2012). Simplified Electrochemical and Thermal Model of $LiFePO_4$-Graphite Li-Ion Batteries for Fast Charge Applications. J. Electrochem. Soc. *159*, A1508–A1519.

37. Khateeb, S.A., Farid, M.M., Selman, J.R., and Al-Hallaj, S. (2004). Design and simulation of a lithium-ion battery with a phase change material thermal management system for an electric scooter. J. Power Sources *128*, 292–307.

38. Zhou, H., Zhou, F., Xu, L., and Kong, J. (2019). QingxinYang. Thermal performance of cylindrical Lithium-ion battery thermal management system based on air distribution pipe. Int. J. Heat Mass Transf. *131*, 984–998.

39. Jiang, Z.Y., and Qu, Z.G. (2019). Lithium–ion battery thermal management using heat pipe and phase change material during discharge–charge cycle: A comprehensive numerical study. Appl. Energy *242*, 378–392.

40. Chen, K.-H., Namkoong, M.J., Mortuza, S.M., Kazemiabnavi, S., Yang, C., Mazumder, J., Thornton, K., Sakamoto, J., and Dasgupta, N.P. (2019). Enabling Fast Charging Lithium-Ion Batteries through the Rational Design of 3-D Anode Architectures. ECS Meeting Abstracts, 243, MA2019-02.

41. Kim, J.-M., and Lee, S.-Y. (2019). 1D Buliding Block Strategies for High Energy Density Li-Ion Batteries. ECS Meeting Abstracts, 276, MA2019-02.

42. Han, M.-C., Zhang, J.-H., Li, Y.-M., Zhu, Y.-R., and Yi, T.-F. (2019). $Li_5Cr_7Ti_6O_{25}$/Multiwalled Carbon Nanotubes Composites with Fast Charge-Discharge Performance as Negative Electrode Materials for Lithium-Ion Batteries. J. Electrochem. Soc. *166*, A626–A634.

43. Nokami, T., Matsuo, T., Inatomi, Y., Hojo, N., Tsukagoshi, T., Yoshizawa, H., Shimizu, A., Kuramoto, H., Komae, K., Tsuyama, H., and Yoshida, J. (2012). Polymer-bound pyrene-4,5,9,10-tetraone for fast-charge and -discharge lithium-ion batteries with high capacity. J. Am. Chem. Soc. *134*, 19694–19700.

44. Kim, N., Chae, S., Ma, J., Ko, M., and Cho, J. (2017). Fast-charging high-energy lithium-ion batteries via implantation of amorphous silicon nanolayer in edge-plane activated graphite anodes. Nat. Commun. *8*, 812.

45. Yamada, Y. (2014). Unusual Stability of Acetonitrile-Based Superconcentrated Electrolytes for Fast-Charging Lithium-Ion Batteries. J. Am. Chem. Soc. *136*, 5039–5046.

46. Du, Z., Wood, D.L., and Belharouak, I. (2019). Enabling fast charging of high energy density Li-ion cells with high lithium ion transport electrolytes. Electrochem. Commun. *103*, 109–113.

47. Han, J.-G., Jeong, M.-Y., Kim, K., Park, C., Sung, C.H., Bak, D.W., Kim, K.H., Jeong, K.-M., and Choi, N.-S. (2020). An electrolyte additive capable of scavenging HF and PF5 enables fast charging of lithium-ion batteries in $LiPF_6$-based electrolytes. J. Power Sources *446*, 227366.

48. Goldar, A., Romagnoli, R., Couto, L.D., Romero, A., Kinnaer, M., and Garone, E. (2020). MPC strategies based on the equivalent hydraulic model for the fast charge of commercial Li-ion batteries. Computers & Chemical Engineering *141*, 107010.

49. Zou, C., Hu, X., Wei, Z., Wik, T., and Egardt, B. (2018). Electrochemical Estimation and Control for Lithium-Ion Battery Health-Aware Fast Charging. IEEE Trans. Ind. *65*, 6635–6645.

50. Lee, A., Vörös, M., Dose, W.M., Niklas, J., Poluektov, O., Schaller, R.D., Iddir, H., Maroni, V.A., Lee, E., Ingram, B., et al. (2019). Photo-accelerated fast charging of lithium-ion batteries. Nat. Commun. *10*, 4946.

51. Hall, D.S., Eldesoky, A., Logan, E.R., Tonita, E.M., Ma, X., and Dahn, J.R. (2018). Exploring Classes of Co-Solvents for Fast-Charging Lithium-Ion Cells. J. Electrochem. Soc. *165*, A2365–A2373.

52. Mai, W., Colclasure, A.M., and Smith, K. (2020). Model-Instructed Design of Novel Charging Protocols for the Extreme Fast Charging of Lithium-Ion Batteries Without Lithium Plating. J. Electrochem. Soc. *167*, 080517.

53. U.S. Department of Energy (2019). XCEL: eXtreme Fast Charge Cell Evaluation of Lithium-ion Batteries (Office of Energy Efficiency & Renewable Energy).

54. Lu, Y., Tikekar, M., Mohanty, R., Hendrickson, K., Ma, L., and Archer, L.A. (2015). Stable Cycling of Lithium Metal Batteries Using High Transference Number Electrolytes. Adv. Energy Mater. *5*, 1402073.

55. Kreuer, K.-D., Wohlfarth, A., de Araujo, C.C., Fuchs, A., and Maier, J. (2011). Single alkaline-ion (Li(+), Na(+)) conductors by ion exchange of proton-conducting ionomers and polyelectrolytes. ChemPhysChem *12*, 2558–2560.

56. Croce, F., Appetecchi, G.B., Persi, L., and Scrosati, B. (1998). Nanocomposite polymer electrolytes for lithium batteries. Nature *394*, 456–458.

57. Videa, M., Xu, W., Geil, B., Marzke, R., and Angell, C.A. (2001). High Li[sup +] Self-Diffusivity and Transport Number in Novel Electrolyte Solutions. J. Electrochem. Soc. *148*, A1352.

58. Suo, L., Hu, Y.-S., Li, H., Armand, M., and Chen, L. (2013). A new class of Solvent-in-Salt electrolyte for high-energy rechargeable metallic lithium batteries. Nat. Commun. *4*, 1481.

59. Doyle, M., Fuller, T.F., and Newman, J. (1994). The importance of the lithium ion transference number in lithium/polymer cells. Electrochim. Acta *39*, 2073–2081.

60. Diederichsen, K.M., McShane, E.J., and McCloskey, B.D. (2017). Promising Routes to a High Li+ Transference Number Electrolyte for Lithium Ion Batteries. ACS Energy Lett. *2*, 2563–2575.

61. Qian, J., Henderson, W.A., Xu, W., Bhattacharya, P., Engelhard, M., Borodin, O., and Zhang, J.-G. (2015). High rate and stable cycling of lithium metal anode. Nat. Commun. *6*, 6362.

62. Yamada, Y., Yaegashi, M., Abe, T., and Yamada, A. (2013). A superconcentrated ether electrolyte for fast-charging Li-ion batteries. Chem. Commun. (Camb.) *49*, 11194–11196.

63. Logan, E.R., and Dahn, J.R. (2020). Electrolyte Design for Fast-Charging Li-Ion Batteries. Trends Chem. *2*, 354–366.

64. Wood, D.L., Li, J., and Daniel, C. (2015). Prospects for reducing the processing cost of lithium ion batteries. J. Power Sources *275*, 234–242.

65. Berckmans, G., Messagie, M., Smekens, J., Omar, N., Vanhaverbeke, L., and Van Mierlo, J. (2017). Cost Projection of State of the Art Lithium-Ion Batteries for Electric Vehicles Up to 2030. Energies *10*, 1314.

66. Zeng, X., Li, M., Abd El-Hady, D., Alshitari, W., Al-Bogami, A.S., Lu, J., and Amine, K. (2019). Commercialization of Lithium Battery Technologies for Electric Vehicles. Adv. Energy Mater. *9*, 1900161.

67. Susarla, N., and Ahmed, S. (2019). Estimating Cost and Energy Demand in Producing Lithium Hexafluorophosphate for Li-Ion Battery Electrolyte. Ind. Eng. Chem. Res. *58*, 3754–3766.

68. Mauger, A., Julien, C.M., Paolella, A., Armand, M., and Zaghib, K. (2018). A comprehensive review of lithium salts and beyond for rechargeable batteries: Progress and perspectives. Mater. Sci. Eng. Rep. *134*, 1–21.

69. Logan, E.R., Tonita, E.M., Gering, K.L., Li, J., Ma, X., Beaulieu, L.Y., and Dahn, J.R. (2018). A Study of the Physical Properties of Li-Ion Battery Electrolytes Containing Esters. J. Electrochem. Soc. *165*, A21–A30.

70. Harlow, J.E., Ma, X., Li, J., Logan, E., Liu, Y., Zhang, N., Ma, L., Glazier, S.L., Cormier, M.M.E., Genovese, M., et al. (2019). A Wide Range of Testing Results on an Excellent Lithium-Ion Cell Chemistry to be used as Benchmarks for New Battery Technologies. J. Electrochem. Soc. *166*, A3031–A3044.

71. Zhang, G., Ge, S., Xu, T., Yang, X.-G., Tian, H., and Wang, C.-Y. (2016). Rapid self-heating and internal temperature sensing of lithium-ion batteries at low temperatures. Electrochim. Acta *218*, 149–155.

72. Ghannoum, A., Norris, R.C., Iyer, K., Zdravkova, L., Yu, A., and Nieva, P. (2016). Optical Characterization of Commercial Lithiated Graphite Battery Electrodes and in Situ Fiber Optic Evanescent Wave Spectroscopy. ACS Appl. Mater. Interfaces *8*, 18763–18769.

73. Ohashi, T., Abe, T., Fukunaga, T., Ogumi, Z., and Matsubara, E. (2020). Analysis of Cathode Reactions of Lithium Ion Cells Using Dynamic Electrochemical Impedance. J. Electrochem. Soc. *167*, 020502.

74. Attia, P.M., Grover, A., Jin, N., Severson, K.A., Markov, T.M., Liao, Y.-H., Chen, M.H., Cheong, B., Perkins, N., Yang, Z., et al. (2020). Closed-loop optimization of fast-charging protocols for batteries with machine learning. Nature *578*, 397–402.

75. Ahmed, S., Bloom, I., Jansen, A.N., Tanim, T., Dufek, E.J., Pesaran, A., Burnham, A., Carlson, R.B., Dias, F., Hardy, K., et al. (2017). Enabling fast charging - A battery technology gap assessment. J. Power Sources *367*, 250–262.

76. Keil, P., and Jossen, A. (2016). Charging protocols for lithium-ion batteries and their impact on cycle life—An experimental study with different 18650 high-power cells. J. Energy Storage *6*, 125–141.

77. Electrek (2020). Tesla files to sell new Model 3 with cheaper lithium iron phosphate batteries. https://electrek.co/2020/05/25/tesla-model-3-cheaper-lithium-iron-phosphate-batteries/.

78. Huang, F.-H. (2020). Understanding user acceptance of battery swapping service of sustainable transport: An empirical study of a battery swap station for electric scooters, Taiwan. Int. J. Sustain. Transport. *14*, 294–307.

79. Hemmati, M., Abapour, M., and Mohammadi-ivatloo, B. (2020). Optimal Scheduling of Smart Microgrid in Presence of Battery Swapping Station of Electrical Vehicles. In Electric Vehicles in Energy Systems: Modelling, Integration, Analysis, and Optimization, A. Ahmadian, B. Mohammadi-ivatloo, and A. Elkamel, eds. (Springer International Publishing), pp. 249–267.

80. Sayarshad, H.R., Mahmoodian, V., and Gao, H.O. (2020). Non-myopic dynamic routing of electric taxis with battery swapping stations. Sustain Cities Soc. *57*, 102113.

81. Billaud, J., Bouville, F., Magrini, T., Villevieille, C., and Studart, A.R. (2016). Magnetically aligned graphite electrodes for high-rate performance Li-ion batteries. Nat. Energy *1*, 16097.

82. Habedank, J.B., Kraft, L., Rheinfeld, A., Krezdorn, C., Jossen, A., and Zaeh, M.F. (2018). Increasing the Discharge Rate Capability of Lithium-Ion Cells with Laser-Structured Graphite Anodes: Modeling and Simulation. J. Electrochem. Soc. *165*, A1563–A1573.